MODELING THERMOHYDROLOGICAL-MECHANICAL BEHAVIOR OF GRANULAR BENTONITE

Chandrika Manepally,[1] Stuart Stothoff,[1] Goodluck Ofoegbu,[1] Biswajit Dasgupta,[1] and Randall Fedors[2]

[1]Center for Nuclear Waste Regulatory Analyses (CNWRA®) Southwest Research Institute® San Antonio, Texas, USA

[2]U.S. Nuclear Regulatory Commission (NRC) Washington, DC

Abstract

Understanding the swelling behavior of materials used in buffers and seals for radioactive waste disposal is important for assessing their barrier capability. Several international radioactive waste disposal programs are actively researching appropriate methods for incorporating the complex coupled thermohydrological (TH) and mechanical processes responsible for the swelling behavior of buffer materials in numerical simulators. This paper discusses efforts to develop a numerical approach to model swelling clays. This approach couples two existing simulators, xFlo (which models TH processes) and FLAC®, with a user-defined constitutive model for unsaturated expansive soils (which models mechanical processes). The numerical development work is described in the context of a laboratory column test, which was designed to study TH conditions in a vertical column of buffer consisting of granular bentonite. The column test features a heater at the bottom (simulating heat from emplaced waste) and both a cooling bath and a source for rewetting (simulating moisture from host rock) at the top. The heater was held at 100 °C [212 °F] and 140 °C [284 °F] in successive stages and then the buffer was wetted at the top of the cell with the heater held at 140 °C [284 °F]. Comparisons of measured temperature and relative humidity at three probe locations with model results indicated that xFlo, in general, is able to represent the evolution of the moisture redistribution in response to heat and hydration. Comparison of water intake measurements indicated that xFlo estimates of imbibition can be improved by considering alternative constitutive relationships such as a power function of saturation. Comparing the measured and calculated axial pressure indicates the mechanical model qualitatively represents the mechanical response.

I. INTRODUCTION

The **De**velopment of **Co**upled Models and Their **Val**idation Against **Ex**periments (DECOVALEX) project is an international collaboration focused on modeling thermal-hydrological-mechanical-chemical (THMC) processes associated with the deep geologic disposal of high-level radioactive waste and spent nuclear fuel. Task B1, in the current phase of DECOVALEX (D2015), is designed to improve understanding of the thermal-hydrological-mechanical (THM) processes in a bentonite buffer and argillaceous host rock at the Mont Terri Underground Research Laboratory (URL), Switzerland. The task is based on three tests: (i) HE-D heating test at Mont Terri (rock only) (ii) laboratory column test on granular bentonite (used as a buffer for the HE-E test) and (iii) HE-E heating experiment at Mont Terri (integrating buffer materials and host rock). The HE-E test is an *in-situ* experiment that is part of the Performance of Engineered Barrier Systems (PEBS) project, funded by the seventh framework project of the European Commission[1]. This paper focuses on the numerical modeling of the laboratory column test conducted by Villar et al[2,3] for granular bentonite.

The laboratory column test was designed to mimic the boundary conditions for the buffer material in the HE-E test by prescribing temperature of the heater at the bottom and a source of hydration (host rock rewetting) at the top. Although the column tests included both granular bentonite and sand/bentonite mixtures, the scope of the DECOVALEX task (and this study) was limited to modeling the column test containing granular bentonite. The granular bentonite used in this test corresponds to a mixture proposed for use in the Swiss disposal concept. This material contains sodium bentonite MX-80 from Wyoming, USA.

The cylindrical cells used in the experiment had a nominal internal diameter of 7 cm [2.8 in] and length of 50 cm [19.7 in] (Fig. 1). The cell walls were made of Teflon®. The outer cell wall was covered with semicylindrical steel shells to avoid deformation of Teflon caused by bentonite swelling. The shells were in turn wrapped in insulation wool to reduce heat loss

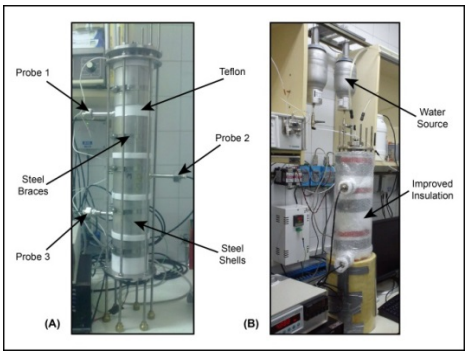

Fig. 1. Column test cell (A) before being wrapped with the insulation material and (B) with improved insulation.

from the cell walls. The bottom part of the cell had a planar stainless steel heater. The upper part consisted of a cooling chamber that circulated water at room temperature, thus ensuring a nearly constant temperature difference between the top and bottom of the column. For the injection phase, water was injected into the column through the upper part of the cell. Synthetic saline water was used for hydration and was a sodium-rich solution with a composition similar to the Opalinus Clay formation pore water. Temperature and relative humidity (RH) were simultaneously measured at three locations: (i) Probe 1 placed at 40 cm [15.7 in] from the bottom, (ii) Probe 2 at 22 cm [8.7 in], and (iii) Probe 3 at 10 cm [3.9 in]. The water intake was measured by means of an electronic load cell measurement system. A ring load cell was used to determine the axial pressure generated during the test.

The heating and hydration phases in the column test were as follows:

(1) Heating Phase 1(0–1,500 hours): the bottom heater temperature was set to 100 °C [212 °F] and the column was insulated with dense foam (termed as "thin insulation" in this paper).

(2) Improved Insulation Phase (1,500–3,524 hours): the bottom heater temperature remained set to 100 °C [212 °F] but the insulation material was replaced to mitigate excessive lateral heat loss. The new insulation was Superwool, covering the entire column, with an additional outer layer of ISOVER material placed from the lowest probe to the countertop (Fig. 1). The combination of Superwool and ISOVER is termed "thick insulation" in this paper.

(3) Heating Phase 2 (3,524–5,015 hours): the heater temperature was increased to 140 °C [284 °F].

(4) Hydration Phase (5,015–19,850 hours): saline water was introduced via an injection tube at the top of the cell with a pressure of 0.01 MPa [0.1 bar] above atmospheric.

II. NUMERICAL MODELING OF THE COLUMN TEST

The THM model is implemented in a two-dimensional (2-D) axisymmetric coordinate system centered along the axis of the column. Four test phases are included in the simulations. Two different simulators were used to represent the coupled THM processes. TH processes were modeled using *xFlo*[4]. Four simulations were performed, with the final state from one simulation used as the initial condition to the next. Geomechanical processes were modeled using FLAC[5]. The *xFlo* model represented the bentonite, heater, Teflon cylinder, steel bands, and insulation. The FLAC model used only the portion of the grid representing the bentonite, without considering other components of the column test. The processes were coupled by passing on *xFlo* output (e.g., temperature, liquid pressure, saturation) to the FLAC model at the end of each heating and hydration phase (Section I). Changes to porosity, estimated by FLAC, were not accounted in the *xFlo* simulations.

II.A. *xFlo* Model

The *xFlo* model[4] is an integrated finite difference model that uses a computational framework similar to the well-known TOUGH model family[6]. *xFlo* considers mass balance of two phases (liquid and gas) and two components (water and air), as well an energy balance.

Equilibrium and saturation constraint equations are employed to reduce the equation set to three fully coupled equations for (i) total mass, (ii) gas mass, and (iii) energy. Air and water are assumed present in both the liquid and gas phases within the bentonite, and *xFlo* solves the fully coupled set of equations for water and air components. Within the other system components (e.g., steel, Teflon), *xFlo* also solves the mass and energy balance equations, but porosity, hydraulic conductivity, and the vapor diffusion coefficient are each set to zero, with the result that thermal conduction is the only process considered.

II.A.I. Input Parameters

Bentonite is modeled as a single continuum with a single value for porosity and saturated hydraulic conductivity. We recognize that swelling in granular bentonite is a complex process, involving interaction of macro and micro pores given its bimodal pore size distribution[7]. Conventional approaches, such as van Genuchten[8] soil water retention relationship and a constant saturated hydraulic conductivity in *xFlo*, were insufficient to match the results. The discussion in the following section details the changes made to some of the *xFlo* input parameters.

Thermal Conductivity: One of the assigned DECOVALEX modeling tasks was to assess the thermal conductivity based on the laboratory observations. We examined a range of thermal conductivity values to assess sensitivity, including a number of different gridding and insulation options. The range of thermal conductivity values were based on laboratory measurements [2,9]. *xFlo* scales thermal conductivity, based on laboratory measurements, from fully unsaturated to fully saturated using the square root of saturation[4].

Water Retention and Relative Permeability Relationship: The moisture retention properties are based on the measured values[10]. The van Genuchten model[8] is used assuming the retention relationship describing capillary pressure is derived at a reference temperature of 20°C [68 °F]. Capillary pressure is subsequently adjusted based on the ratio of surface tensions under actual and reference temperatures. Vapor transport in bentonite turned out to be sensitive to this temperature-dependent adjustment under the moisture and temperature conditions in the experiment. In *xFlo*[4], relative permeability in the liquid phase is related to liquid saturation by combining van Genuchten's relation with Mualem's model[11].

Hydraulic Conductivity: Moisture redistribution occurs primarily by vapor transport in the thermal phase, but liquid transport dominates in the injection phase. Therefore, the precise value of hydraulic conductivity is not important in the thermal phase, but is important in the injection phase. The nominal saturated hydraulic conductivity during the thermal phase is based on interpolation of laboratory experiments[12].

Klinkenberg Parameter: The gas conductivity was increased using a Klinkenberg[13] parameter (9×10^{11} Pa [1.3×10^{8} psi]) implemented by multiplying the gas relative permeability by a scaling factor[6]. This approach provided a convenient way to adjust the gas conductivity independent of the liquid (intrinsic) permeability. Our numerical calculations indicate that thermal phase simulations are insensitive to the Klinkenberg parameter when it is at least 4 or 5 orders of magnitude larger than the atmospheric pressure.

Water Properties: Water properties are assumed to be described by National Institute of Standards and Technology Steam Table (e.g., http://enpub.fulton.asu.edu/ece340/pdf/steam_tables.PDF). The gas phase is assumed to be governed by the ideal gas law. Dissolved air is assumed to be in equilibrium with the gas phase through Henry's Law. Water vapor is assumed to be in equilibrium with the liquid phase, considering temperature- and capillary-pressure-dependent vapor pressure lowering using the Kelvin equation.

II.A.2. Boundary and Initial Conditions

Several thermal-related parameters were measured in the laboratory experiment: (i) computer controlled heater temperature, (ii) energy flux to the heater, (iii) temperatures at three probes, (iv) approximate cooling-bath temperature, and (v) laboratory temperature (during the injection phase). The experiment also measured RH at the three probes, cumulative inflow of water during injection, and axial pressure at the top of the column.

In the *xFlo* model, all materials bordering the bentonite are assumed impermeable except the injection cylinder (during the injection phase) and the porous plate (assumed properties). The injection cylinder overlaps the innermost two grid cells at the top of the bentonite. During the injection phase, the injection cylinder was assumed to provide deaerated water at a pressure corresponding to atmospheric pressure plus 0.01 MPa [0.1 bar] (the pressure surcharge in the bladder) plus hydrostatic pressure from 90 cm elevation difference between the top of the water in the bladder to the top of the bentonite, corresponding to a pressure of 0.12015 MPa [17.4 psi]. Gas was allowed to exit through the injection cylinder. The inlet water is assumed to be at room temperature {22 °C [71.6 °F]}. Based on available data[2], the initial bentonite saturation was assumed to be 0.22. Since the reported room temperatures didn't vary more than 2 °C [3.6 °F], a constant room temperature of 22 °C [71.6 °F] was assumed.

The long and thin geometry of the bentonite column suggests the temperature field within the

bentonite should be approximately one-dimensional (1-D), especially with the relatively uniform temperatures applied at the top and bottom. However, thermal analysis should also consider the effect of conduction within the steel bands supporting the Teflon cylinder and heat loss to the atmosphere. To examine the effect of different thermal boundary condition treatments, we developed a thermal-only model that considered the experimental apparatus in detail using COMSOL Multiphysics[14] (hereafter called the COMSOL model). This provided guidance for selection of the domain and boundary conditions used for *xFlo* thermal analyses.

The COMSOL model provided several insights into the thermal processes including: (i) the steel shells carry a much larger fraction of the total axial heat flux than the bentonite as they are 50 to 140 times as conductive as bentonite; (ii) much of the supplied energy is lost below the heater element; and (iii) the boundary conditions outside the insulation should result in insulation surface temperatures between room temperature (maximum heat loss) and the surface-to-ambient-radiation temperature (minimum heat loss, because it does not consider cool air moving past the surface). Surface temperatures are much higher than room temperature near the heater with thin insulation, but are quite similar with thick insulation. Reasonably good matches to the observed temperatures were obtained with the bentonite thermal conductivity set to 0.33 W/m/K [0.19 BTU/h/ft/F] assuming surface-to-ambient radiation losses, once heat loss below the heater was adjusted to match the observed heater temperatures. The lowest steel reinforcing band collects energy from the side of the heater element (and bottom, in thick insulation scenarios) and transports it above the heater. This creates a thermal divide below the actual heater element. The central 2.5 cm [0.98 in] of the steel heater where it contacts the bentonite is essentially at the same temperature as the heater element. Temperatures along the top and outer edges of the steel heater generally are the same to within 1.5 °C [2.7 °F]. For the purposes of modeling mass transport in the bentonite, it should be adequate to (i) make the bottom of the domain correspond to the thermal divide elevation and (ii) assign the heater temperature to the inner 3 cm [1.2 in] of the bottom of the domain. This was the strategy used for *xFlo* simulations.

With the insights gained from the COMSOL modeling, the *xFlo* model was designed such that (i) the top of the bentonite is set to room temperature of 22 °C [71.6 °F]; (ii) the domain extends 1.5 cm [0.6 in] below the bentonite, including projections of the steel heater, the Teflon cylinder, the steel reinforcing band, and the insulation; (iii) the temperature at the bottom of the domain is either 100 or 140 °C [212 or 284 °F] within a radius of 3 cm [1.2 in] from the axis. The *xFlo* model does not include a surface-to-ambient radiation boundary condition akin to the COMSOL boundary condition, so the boundary temperature outside the insulation was set to room temperature.

Some of the sensitivity tests applied an artificially small thermal conductivity to reduce heat loss over the lower portion of the thin insulation (from the top of the lowest steel band to the bottom of the domain), approximately mimicking surface-to-ambient radiation.

II.B. Mechanical Analysis (FLAC) Model

The mechanical model uses the temperature, liquid saturation, and gas pressure calculated in the thermal-hydrological model as inputs to calculate the mechanical response in terms of deformation (porosity change) and pressure. The mechanical analysis was performed using the user defined MCUS (modified CAM-clay model for unsaturated soils) constitutive model[14] implemented for numerical computation using FLAC. As Ofoegbu, et al.[15] described, MCUS is based on the Bishop principle of effective stress to represent the effects of suction on soil stress, incorporates the effects of suction and compaction on mechanical properties, and uses stress-strain relationships based on elasto-plasticity.

II.B. I Input Parameters

The Bishop parameter χ is set equal to the effective saturation (S_e) and is described as a function of suction (s). The resulting suction contribution to soil pressure [i.e., suction pressure (p_s)] is calculated as a product of χ and s. The suction pressure was combined with the value of preconsolidation pressure for saturated conditions (P_{c0}) based on data[10] to obtain the preconsolidation pressure model shown in Fig. 2. As Ofoegbu, et al.[15] described, the soil bulk modulus (K) is a function of pressure (p) and void ratio, which translates to a variation with s (Fig. 3). The K-p relationship is influenced by P_{c0}, the unload-reload slope (denoted κ_r), and a fitting parameter (K_∞) that represents an asymptotic maximum bulk modulus of 50 MPa [7,250 psi]. An examination of relationships among the various parameters indicated this value to be appropriate. A slightly smaller or larger value could work but could result in inappropriate values for other parameters. The

additional input parameters for the FLAC model are listed in Table 1.

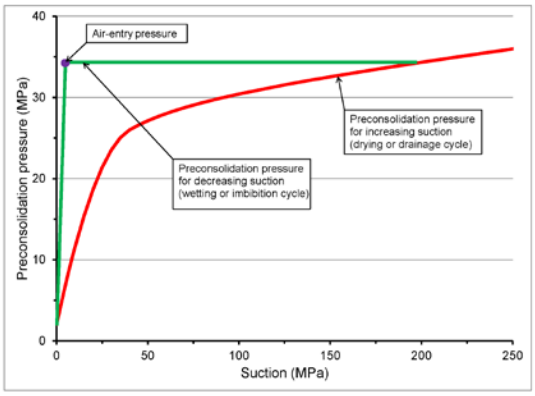

Fig. 2. Preconsolidation pressure P_c versus suction s model based on P_{co} = 2 MPa [For saturated condition, based on data from Rizzi, et al.[10]] and suction pressure.

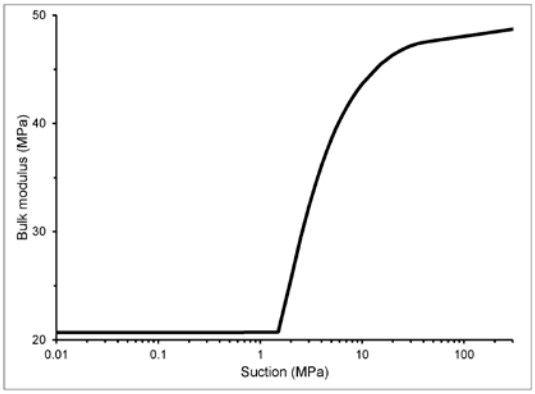

Fig 3. Bulk modulus K versus suction s model (based on K-p relationship[14] and parameter values described in this paper).

III RESULTS

III.A. Thermal Hydrological Analyses

Thermal hydrological (TH) analyses are conveniently broken into the thermal period while the column is heated, and the injection phase when mass is allowed to enter while heating continues. The thermal period consists of three phases (described previously in Section I) simulated separately: (i) Heating Phase 1, (ii) Improved Insulation Phase, and (iii) Heating Phase 2, for a total of 5,015 hours. The injection phase is the next 14,835 hours. The last two thermal phases and the injection phase are initialized using the final state from the previous simulation.

The wetting saturation profiles, estimated *xFlo*, suggest the steel reinforcement (because of its high thermal conductivity) perturbs the temperature field sufficiently to locally enhance condensation where heat is drawn from the bentonite. This behavior was noted between the top two probes. The same behavior also occurred lower in the profile, but was erased as the drying zone propagated upward.

Fig. 4 shows the time history of the temperature and RH during the thermal period at the three probe locations. The symbols plotted for RH and temperature are the laboratory measurements. Calculated temperatures are slightly below the measured values during Heating Phase 1 and slightly exceed the observed temperatures in later phases. The indicator of moisture state (i.e., RH), suggests the *xFlo* estimates at Probe 3 match the observations well during the Heating Phase 1. However, during the later phases of heating, *xFlo* estimates of RH indicate drying in the bentonite relative to what was observed in the experiment at Probe 3. Artificially adjusting the boundary conditions or thermal conductivity to better match the temperatures tends to bring the RH closer to the measured values.

During the infiltration period, the *xFlo* calculations show essentially no change in the temperature profile (Fig. 5). The time history of the measured RH suggests the observed wetting front is smeared relative to the *xFlo*-calculated wetting front. Water moves to depth slower (relative to observations) at low saturations in the *xFlo* calculations. Sensitivity analyses indicated the inclusion of the porous plate in *xFlo* had a significant effect on the estimated imbibition rate (mass inflow), as shown in Fig. 6. An *xFlo* simulation without a porous plate required the saturated hydraulic conductivity be increased by a factor of 20 to match the observations (the curve labeled "*xFlo*: k × 20, no plate" in Fig. 6). A comparison of these curves with the observed mass intake indicates the actual inflow is characteristic of a diffusion-like process, because the rate of inflow scales with $t^{-0.5}$. However, the *xFlo*-calculated inflow is essentially constant over time, characteristic of an advection dominated process (gravity drainage). Sensitivity studies suggest the simulated inflow rate is dominated by gravity drainage, even with much reduced saturated hydraulic conductivity.

TABLE 1. FLAC Input Parameters

Bentonite Property	Value	Comments
Reference specific volume ($v_{ref\,0}$)	$v_{ref\,0} = 2.0 - \frac{s}{175 + 3.7s}$	Function of suction (s)
Unload-reload slope (κ_r)	$\kappa_r = 0.15 - \frac{s}{5000 + 25s}$	Function of suction (s)
Virgin compression slope (λ_s)	$\lambda_s = 0.23 + \frac{s}{100 + 20s}$	Function of suction (s)
Unit swelling potential (α_{CW})	α_{CW} *decays towards* 0.05 *for* $\theta_l \geq 0.12$ $\alpha_{CW} = 1$ *for* $0.075 \leq \theta_l \leq 0.12$ $\alpha_{CW} = 0$ *for* $\theta_l \leq 0.075$	Function of moisture content
Thermal expansivity (α_{Th})	$\alpha_{Th} = 10^{-5}\ /^0C$	

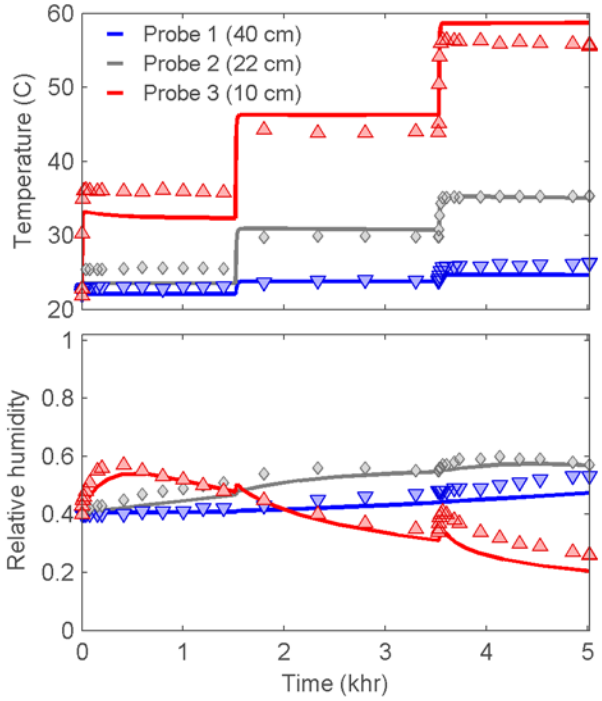

Fig. 4. Time history of temperature and RH at probe locations over the thermal phase. Symbols indicate laboratory measurements and lines indicate model results.

Further evaluation indicated the imbibition rate was controlled by the relative permeability–saturation relationship at the wetting front and not by the saturated permeability. Using other constitutive relationships, such as a power function of saturation[5], may improve the match. The calibrated saturated permeability will depend on the relative permeability–saturation relationship used in the simulation.

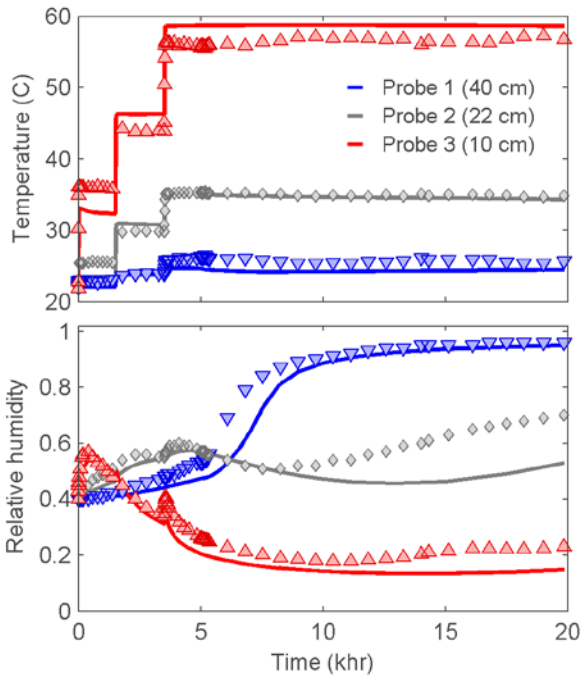

Fig. 5. Time history of temperature and RH at probe locations over the thermal and injection phases. Symbols indicate laboratory measurement and lines indicate model results.

III.B. Geomechanical Analyses

The geomechanical model was used to calculate pressure histories within the bentonite column. As Fig. 7 shows, the measured axial pressure varied between 0.1–0.2 MPa [14.5–29 psi] for the first 5,000 hours (heating phase) of the test, increased rapidly to approximately 1 MPa [145 psi] during the first 500 hours of infiltration, and increased slowly

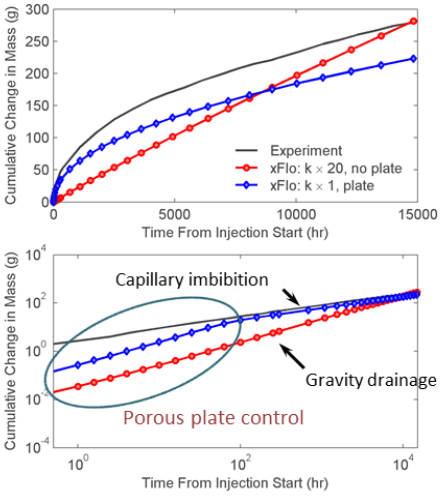

Fig. 6. Time history of cumulative inflow over the injection phase.

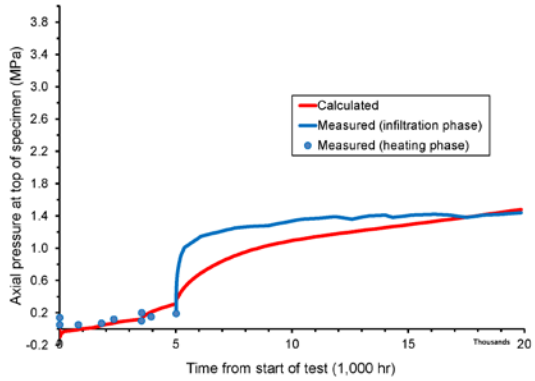

Fig. 7. Calculated and measured axial pressure histories at the top of the bentonite column over the thermal and injection phases.

toward 1.4 MPa [203 psi] during the remainder of the infiltration phase.

Our calculations indicate the axial pressure was controlled by moisture redistribution throughout the test. The contribution of thermal expansion to the axial pressure appears negligible. The calculated axial pressure during the thermal and infiltration phases matches the measured behavior overall. Further calibration of the mechanical parameters relevant to swelling pressure may yield a better match.

III.C. Conclusions from the Column Study

Several observations and conclusions can be drawn from the progress on modeling the bentonite pellet column test.

The thermal conductivity for bentonite is difficult to determine from the experimental measurements because of uncertainties related to heat loss and the dominant effect of highly conductive steel reinforcement bands in the laboratory setup. The COMSOL and *xFlo* models suggest the bentonite thermal conductivity is approximately 0.33 W/m/K [0.19 BTU/h/ft/F].

Thermal phase measurements could not be matched unless the gas relative permeability was increased by several orders of magnitude in the dry media. The Klinkenberg relationship was used to scale gas permeability and provides a convenient mechanism for scaling gas phase transport.

During the infiltration phase, *xFlo* was unable to represent the observed response of swelling clays in response to imbibition. The simulated inflow rate is dominated by gravity drainage, even with much reduced saturated hydraulic conductivity. Further evaluation indicated the imbibition rate was controlled by the relative permeability–saturation relationship at the wetting front and not by the saturated permeability. *xFlo* currently uses the van Genuchten relationship and does not capture the imbibition behavior observed in the column test adequately. Using other constitutive relationships, such as a power function of saturation[5] may improve the match. The calibrated saturated permeability will depend on the relative permeability–saturation relationship used in the simulation.

The geomechanical model qualitatively represents the observed behavior (i.e., the changes in axial pressure). Further calibration of the mechanical parameters relevant to swelling pressure may yield a better match.

ACKNOWLEDGMENTS

This abstract is an independent product of the CNWRA and does not necessarily reflect the view or regulatory position of the NRC. The NRC staff views expressed herein are preliminary and do not constitute a final judgment or determination of the matters addressed or of the acceptability of any licensing action that may be under consideration at the NRC.

REFERENCES

1. I. Gaus, K. Wieczorek, K. Schuster, B. Garitte, R. Senger, R., Vasconcelos and J. C. Mayor "EBS Behaviour Immediately After Repository Closure in a Clay Host Rock: HE-E Experiment (Mont Terri URL)". Geological Society. London. Special Publications. Doi 10.1144/SP400.11. 2014.
2. MV. Villar, P.L. Martin, R. Gomez-Espina, F.J. Romero, and J.M. Barcala. "THM Cells for the HE-E Test: Setup and First Results." PEBS Report D2.2.7a. Madrid, Spain: Long-Term Performance of Engineered Barriers Systems Project. 2012.
3. M.V. Villar, P.L. Martin, R. Gomez-Espina, and F.J. Romero. "Long-term THM Tests Reports: THM Cells for the HE-Test: Update of Results Until February 2014." PEBS Report D2.2-7.3. Madrid, Spain: Long-Term Performance of Engineered Barriers Systems Project. 2014.
4. S. Painter. "*xFlo* Version 1.0β User's Manual." San Antonio, Texas: Center for Nuclear Waste Regulatory Analyses. 2006.
5. Itasca Consulting Group. "FLAC V 7.0, Fast Lagrangian Analysis of Continua, User's Guide." Minneapolis, Minnesota: Itasca Consulting Group. 2011.
6. K. Pruess, C. Oldenburg, and G. Moridis. "TOUGH2 User's Guide, Version 2.1." Report LBNL–43134. Berkeley, California: Lawrence Berkeley National Laboratory. 2012.
7. A. Seiphoori, A. Ferrari, and L. Laloui. "An Insight Into the Water Retention Behaviour of MX 80 Granular Bentonite." International Conference on the Performance of Engineered Barriers. February 6–7, 2014. Hannover, Germany. 2014.
8. M.T. van Genuchten. "A Closed-Form Equation for Predicting the Hydraulic Conductivity of Unsaturated Soils." Soil Science Society of America Journal. Vol. 44. pp. 892–898. 1980.
9. K. Wieczorek and R. Miehe. "Measurement of Thermal Parameters of the HE-E Buffer Materials." Deliverable D2.2-5 of the PEBS Project. European Commission. 2011.
10. M. Rizzi, A. Seiphoori, A. Ferrari, D. Ceresetti, and L. Laloui. "Analysis of the Behaviour of the Granular MX-80 Bentonite in THM-Processes." AN 12-102. Wettingen, Switzerland: Nagra. 2012.
11. Y. Mualem. "A New Model for Predicting the Hydraulic Conductivity of Unsaturated Porous Media." *Water Resources Research.* Vol. 12, No. 3. pp. 513–522. 1976.
12. O. Karnland, U. Nilsson, H. Weber, P. Wersin. "Sealing Ability of Wyoming Bentonite Pellets Foreseen as Buffer Material—Laboratory Results." Physics and Chemistry of the Earth. Vol. 33. pp. S472–S475. 2008.
13. L.J. Klinkenberg. "The Permeability of Porous Media to Liquids and Gases." API Drilling and Production Practice. pp. 200–213. 1941.
14. COMSOL AB (2012) COMSOL Multiphysics user's guide, version 4.3a
15. G. Ofoegbu, B. Dasgupta, C. Manepally, H. Basagaoglu, and R. Fedors. "Modeling Swelling and Swelling Pressure in Expansive Clays." 2013 International High-Level Radioactive Waste Management Conference, Albuquerque, New Mexico, April 28–May 2, 2013. La Grange Park, Illinois: American Nuclear Society. 2013.